A NOVEL SELECTIVE ACTIVE NOISE CONTROL ALGORITHM TO OVERCOME PRACTICAL IMPLEMENTATION ISSUE

DongYuan Shi[*]*, Bhan Lam and Woon-Seng Gan*

Digital Signal Processing Laboratory, School of Electrical and Electronic Engineering,
Nanyang Technological University, SINGAPORE

ABSTRACT

Selective active noise control (SANC) is a method to select a pre-trained control filter for different primary noises, instead of using conventional real-time computation of the control filter coefficients. SANC has the advantage of improving the robustness of control filter while reducing the computational complexity. This paper presents a practical strategy in choosing a suitable control filter based on the frequency-band-match mechanism implemented in a partitioned frequency domain filter structure. Both simulation and real-time experiment are carried out validate the noise reduction performance of the SANC compared to the conventional FxLMS algorithm.

Index Terms— Active Noise Control, Real-Time Implementation, Digital Signal Processing, FxLMS algorithm.

1. INTRODUCTION

Active noise control (ANC) system employs a secondary source to generate anti-noise to cancel out the unwanted noise that enters into the listening environment [1]. The underlying signal processing mechanism behind ANC is the filtered-x least mean square (FxLMS) algorithm and its variants. FxLMS is an adaptive algorithm that updates a control filter's coefficients in real time with the aim of generating an anti-noise signal, which matches the primary noise in space and time at the desired location. Although ANC is ubiquitous in headphones [2, 3] and modern automobiles, its application in larger three-dimensional spaces has been limited. Active control of broadband noise in large spaces requires multiple control sources that operate at higher sampling frequencies with longer control filter. This improves the coherence of reference and error sensors and satisfies causality, which are important factors for good noise control performance [4, 5]. To realize large multichannel ANC systems, high-performance processors, such as multi-core DSP processors, FPGA [6], and GPU [7] are required, which increases cost and complicates the programming effort. These processing limitations undermine its potential applications (e.g., in building windows [8, 9, 10], large dimension ducts or closure rooms, active noise barriers) and deteriorate the system stability.

There are many different approaches to reduce the computational burden for large structure ANC systems [11, 12]. One such solution is the use of a fixed filter to control different types of noise sources and orientations [13]. The coefficients of the control filter are first pre-trained for different ANC setups, and then these trained (fixed) coefficients of the control filter can be deployed in the actual operation using low-cost analog and digital processing units. A point in case is from ANC headphones, which generally use analog filters by pre-tuning its gain and phase response to handle different types of noise environments [14, 15]. Furthermore, this fixed-coefficient filter ANC usually cannot change the control filter's coefficients for different primary noise sources on the fly, which will result in poor noise reduction performance.

In this paper, we propose a practical, computationally efficient strategy to adapt to the different primary noise types. This method is known as the selective active noise control (SANC) and uses the frequency-band-match approach to match the incoming noise frequency patterns with the spectrum of the control filter. The pre-trained control filter that matches to the primary noise signature will be selected as the control filter for the ANC system.

2. FREQUENCY-BAND-MATCH METHOD

SANC is based on the frequency-band-match method to select pre-trained control filter coefficients to cancel a specific type of primary noise. A pre-trained filter whose training signal has the same frequency band as the primary noise will be selected as the control filter. The block diagram of the single channel feedforward ANC is shown in Fig. 1. In the training phase, a broadband training signal $X_0(\omega)$ is input as a reference signal

$$X_0(\omega) = T_0(\omega) rect(\frac{\omega - \omega_0}{2B_0}), \tag{1}$$

where $T_0(\omega)$ is a univalent and conjugate symmetry function [16] for ω. ω_0 and B_0 are the central frequency and bandwidth

[*]Thanks to Yanlin Li for supporting.

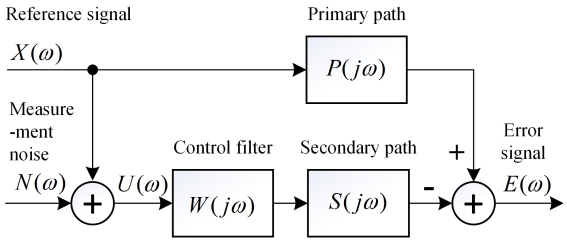

Fig. 1. Block diagram of single channel feedforward ANC.

of the training signal, respectively. The rectangular function can be written as

$$rect\left(\frac{\omega-\omega_0}{2B_0}\right) = u(\omega-\omega_0+B_0) - u(\omega-\omega_0-B_0), \quad (2)$$

where $u(\omega)$ is a Heaviside step function. Hence, the power spectral density of filtered signal $r_0(n) = s(n) * x_0(n)$ ($*$ denotes the convolution operation) can be stated as

$$S_{r_0r_0}(\omega) = S_{x_0x_0}|S(j\omega)|^2 rect\left(\frac{\omega-\omega_0}{2B_0}\right), \quad (3)$$

where $S(j\omega)$ is the transfer function of the secondary path, and $S_{x_0x_0}$ equals to $E\{X_0^*(\omega)X_0(\omega)\}$. The cross-spectral density of the filtered signal $r_0(n)$ and disturbance noise $d(n)$ is expressed as

$$S_{r_0d_0}(\omega) = S_{x_0x_0}(\omega)S^*(j\omega)P(j\omega)rect\left(\frac{\omega-\omega_0}{2B_0}\right), \quad (4)$$

where $P(j\omega)$ is the transfer function of the primary path. The optimal control filter [4, 5] of the trained signal at $\omega \in [\omega_0 - B_0, \omega_0 + B_0]$ is stated as

$$W_{opt}^0(j\omega) = \frac{S_{r_0d_0}(\omega)}{S_{r_0r_0}(\omega)} = \frac{P(j\omega)}{S(j\omega)}. \quad (5)$$

The recursive algorithms, such as FxLMS algorithm, can be used to compute the $W_{opt}^0(j\omega)$ outside the frequency of interest (i.e., $(-\infty, \omega_0 - B_0) \cup (\omega_0 + B_0, \infty)$). If the initial coefficients of $W^0(j\omega)$ are assumed to be zeros, the optimal control filter would be

$$W_{opt}^0(j\omega) = 0, \ (-\infty, \omega_0 - B_0) \cup (\omega_0 + B_0, \infty). \quad (6)$$

By combining (5) and (6), the optimal control filter is rewritten as

$$W_{opt}^0(j\omega) = \frac{P(j\omega)}{S(j\omega)} rect\left(\frac{\omega-\omega_0}{2B_0}\right). \quad (7)$$

Next, we assume that the primary noise is a broadband noise with the central frequency of ω_1 and bandwidth B_1 ($B_1 \leq B_0$),

$$X_1(\omega) = T_1(\omega) rect\left(\frac{\omega-\omega_1}{2B_1}\right). \quad (8)$$

where $T_1(\omega)$ has the same property as $T_0(\omega)$. Based on the same procedure as $X_0(\omega)$, the optimal control filter of the primary noise $X_1(\omega)$ can be derived as

$$W_{opt}^1(j\omega) = \frac{P(j\omega)}{S(j\omega)} rect\left(\frac{\omega-\omega_1}{2B_1}\right). \quad (9)$$

As depicted in Fig. 1, the reference signal is given by

$$U(\omega) = X_1(\omega) + N(\omega), \quad (10)$$

where $N(\omega) \sim N(0, \frac{N_0}{2})$ is a white Gaussian noise, which is the sum of quantization noise, channel noise from the primary source to reference sensor, and electronic components noise. If we apply $W_{opt}^0(\omega)$ as the control filter in Fig. 1 to cancel the primary noise, the error signal is written as

$$\begin{aligned} E(\omega) &= X_1(\omega)P(j\omega) \\ &\quad - (X_1(\omega) + N(\omega))\, W_{opt}^0(j\omega)S(j\omega). \end{aligned} \quad (11)$$

Hence, when $\omega_0 = \omega_1$, its power spectral density can be derived as

$$\begin{aligned} S_{e_1e_1}(\omega) &= S_{e_1e_1}(\omega)_{min} rect\left(\frac{\omega-\omega_0}{2B_1}\right) \\ &\quad + \frac{N_0}{2}\left|\frac{P(j\omega)}{S(j\omega)}\right|^2 \left[rect\left(\frac{\omega-\omega_0}{2B_0}\right)\right. \\ &\quad \left. - rect\left(\frac{\omega-\omega_0}{2B_1}\right)\right], \end{aligned} \quad (12)$$

where

$$\begin{aligned} S_{e_1e_1}(\omega)_{min} &= S_{d_1d_1}(\omega) \\ &\quad - \frac{|S_{r_1d_1(\omega)}|^2}{S_{r_1r_1(\omega)}} + \frac{N_0}{2}\left|\frac{P(j\omega)}{S(j\omega)}\right|^2, \end{aligned} \quad (13)$$

and $S_{d_1d_1}(\omega) = E\{D^*(\omega)D(\omega)\}$. $S_{e_1e_1}(\omega)_{min}$ is the PSD of the error signal when the control filter arrives at its optimal solution $W_{opt}^1(j\omega)$. If we assume that the primary path and secondary path are just pure delays with unit gain, the mean square error (MSE) is derived by integrating (12)

$$\begin{aligned} E\{e(n)^2\} &= \frac{1}{2\pi}\int_{-\infty}^{\infty} S_{e_1e_1}(\omega)d\omega \\ &= J_{min} + \frac{N_0}{2\pi}(B_0 - B_1), \end{aligned} \quad (14)$$

where

$$J_{min} = \frac{1}{2\pi}\int_{-\infty}^{\infty} S_{e_1e_1}(\omega)_{min}d\omega, \quad (15)$$

which is the minimal square error (MMSE) of the Wiener-Hopf solution [17]. In (14), if the bandwidth B_0 equals to B_1, the MSE of SANC is same as the MMSE of the FxLMS. Therefore, if the control filter of SANC has the same frequency band with primary noise, it will achieve the same noise reduction performance as the FxLMS.

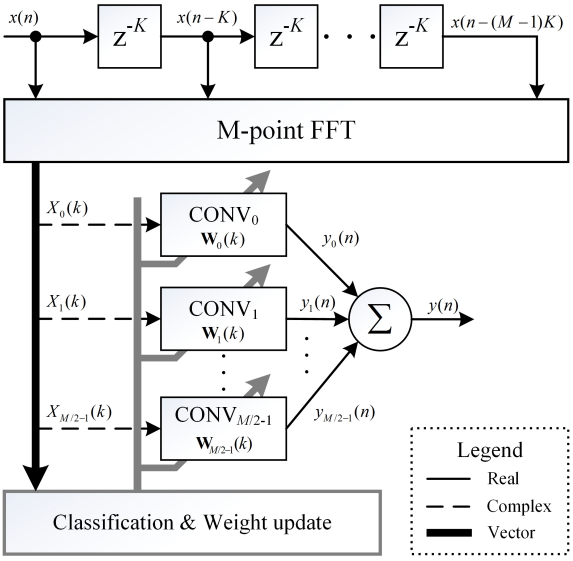

Fig. 2. Overall block diagram of SANC.

3. PROPOSED SELECTIVE ACTIVE CONTROL ALGORITHM

To further reduce computational complexity, com-partitioning frequency domain adaptive filter (FDAF) [18, 19, 20, 21] is modified to form a delayless selective ANC as shown in Fig. 2. SANC consists of three main processes: (1) comb-partitioning FFT, (2) convolution, and (3) classification and weight update.

In the comb-partitioning FFT, an M-point FFT is applied to complete an N-point frequency domain transform [20, 21] ($M < N$). The reference signal $x(n)$ is first input into an $(N-K)$ taps delay line ($M = N/K$). Hence, the partitioned input vector is defined as

$$\mathbf{x}(n) = [x(n), x(n-K), \ldots, x\,(n-(M-1)K)]^{\mathrm{T}}, \quad (16)$$

and its Fourier transform is stated as

$$\mathbf{X}(k) = [X_0(k), X_1(k), \ldots, X_{M-1}(k)]^{\mathrm{T}}, \quad (17)$$

where T denotes the transposition. Then, we can derive the output $y_m(n)$ of the m-th convolution unit (shown in Fig. 3) as

$$y_m(n) = real\Big\{ \sum_{q=0}^{K-1} W_{m,q}(k) X_m(k - qM) \Big\}, \quad (18)$$

Since the input signal is real signal, its frequency spectrum is conjugate symmetry, and the output $y(n)$ of the control filter is given by

$$y(n) = \sum_{m=0}^{M/2-1} y_m(n) \quad (19)$$

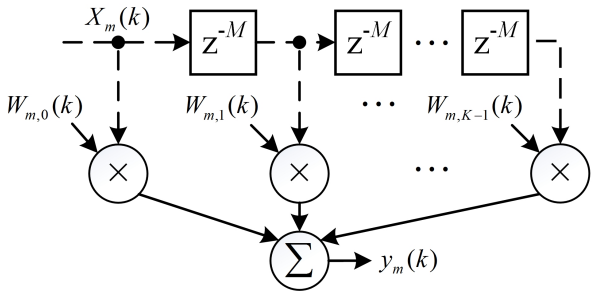

Fig. 3. The m-th convolution block, $\mathrm{CONV_m}$ in SANC.

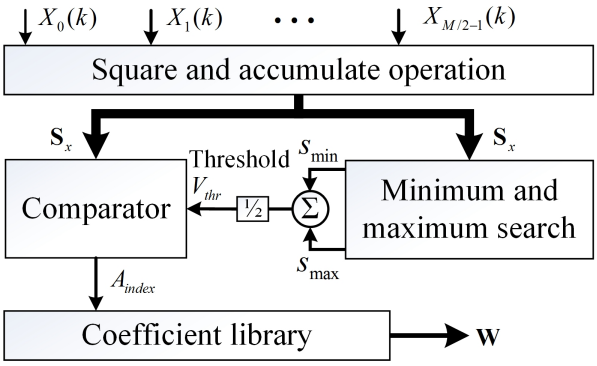

Fig. 4. The classification and weight update part in SANC.

The SANC algorithm adopts the frequency-band-match for classification, and continuously updates the coefficients of the control filter, at every L iterations, as shown in Fig. 4. The classification estimate the power spectrum of the primary noise $X(k)$ by accumulating its FFT result L times

$$\begin{aligned}\mathbf{S}_x = \Bigg[&\sum_{t=0}^{L-1} \big\|X_0(k-t)\big\|^2, \sum_{t=0}^{L-1} \big\|X_1(k-t)\big\|^2, \ldots, \\ &\sum_{t=0}^{L-1} \big\|X_{\frac{M}{2}-1}(k-t)\big\|^2 \Bigg]^{\mathrm{T}}.\end{aligned} \quad (20)$$

A threshold is derived by the average of the minimum scalar s_{min} and the maximum scalar s_{max} of the vector $\mathbf{S}_x$ in (20).

$$V_{thr} = \frac{s_{min} + s_{max}}{2}, \quad (21)$$

It is compared with the vector $\mathbf{S}_x$, which results a $\frac{M}{2}$ bit binary A_{index}

$$A_{index,i} = \begin{cases} 0, & \text{for } S_{x,i} < V_{thr},\ i = \mathbb{Z}^+ \le M/2 \\ 1, & \text{for } S_{x,i} \ge V_{thr},\ i = \mathbb{Z}^+ \le M/2, \end{cases} \quad (22)$$

where $A_{index,i}$ is the i-th bit of A_{index}, and $S_{x,i}$ is the i-th element of $\mathbf{S}_x$. In the final stage, the coefficient library

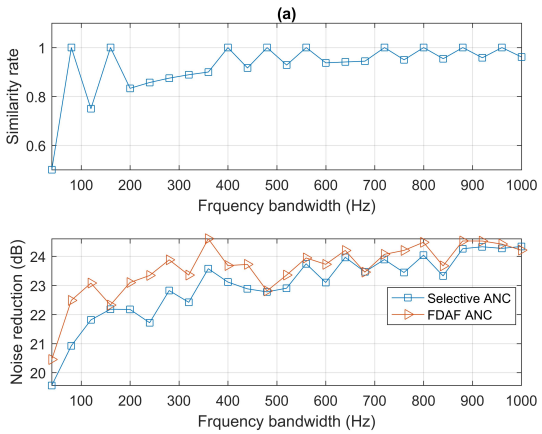

Fig. 5. (a). Similarity ratio of the selected filter and primary noise; (b). Noise reduction of SANC and FDAF ANC for the different frequency-band noises.

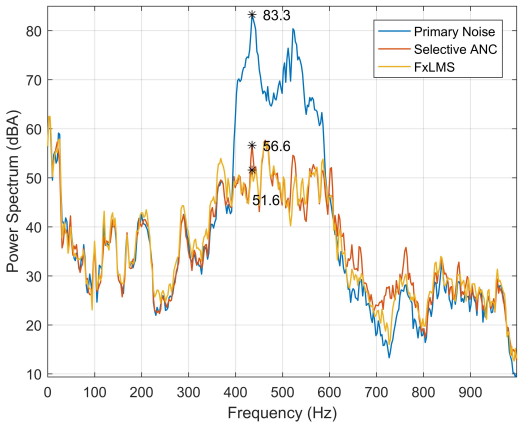

Fig. 6. Power spectrum of the primary noise and the error signal of SANC and FxLMS algorithm.

selects a set of coefficients $\mathbf{W}$ according to the index A_{index}. The coefficients in the library is attained by pre-training the control filter by different broadband noises [20].

4. SIMULATION AND EXPERIMENT

In this section, an ANC simulation is carried out to examine the performance of the SANC algorithm compared to the conventional FxLMS algorithm. The primary path and secondary path are measured from an air duct, and the system sampling frequency is 8 kHz. The primary noise has a central frequency of 2 kHz, and its frequency bandwidth gradually increased from 40 Hz to 1 kHz. $N = 256$ and $K = 4$ are used in the SANC. To test the performance of the classification and weight update unit, a similarity ratio is introduced as

$$SR = \frac{B_{over}}{max\left(B_0, B_1\right)}, \tag{23}$$

where B_{over} is the bandwidth overlap between the primary noise and selected filter, whose frequency bandwidths are B_0 and B_1, respectively. $max(\cdot)$ is choosing the larger one of the two numbers. The similarity rate of the control filters chosen by this unit for different primary noises is illustrated in Fig. 5 (a). The noise reduction performance of SANC and frequency domain adaptive (FDAF) ANC for the primary noise with different bandwidth is shown in Fig. 5. When the SR is equal to 1, the SANC almost has the same noise reduction performance as the FDAF ANC, which confirms the conclusion of section II.

To verify the performance of SANC, it is implemented on the NI PXIe 8135 platform and compared to FxLMS in a duct. The system sampling frequency is 16 kHz, the filter length N of the SANC and FxLMS is 1024, K and L are chosen as 16 and 256, and the length L_s of the secondary path model is 512. FxLMS uses $(2N+L_s) = 2560$ multiplications and additions at each iteration, while SANC just uses $(N + \frac{N}{K}\log\frac{N}{K} + \frac{N}{LL_s}) = 1408$ operations. The frequency range of primary noise is from 400 to 600 Hz. The noise reduction of the SANC and FxLMS are 21.9 dB and 23 dB, respectively, as shown in Fig. 6.

5. CONCLUSION

This paper revisits and proves the frequency-band-match method for the implementation of selective ANC (SANC), in which the algorithm will choose a suitable pre-trained control filter based on the frequency band of the primary noise rather than adaptively updating the coefficients of the control filter. This paper also proposed a SANC technique based on frequency domain adaptive filter (FDAF) algorithm, which significantly reduces the computational burden of FFT. A new classification and weight update module in the algorithm efficiently realizes the adjustment of the control filter for different primary noise in real-time. To verify this SANC algorithm, we implemented it in NI PXIe-8135 and tested its performance in an ANC duct. The result shows it can achieve 21.9 dB noise reduction for a broadband noise at the low frequency.

6. ACKNOWLEDGEMENT

This material is based on research/work supported by Singapore Ministry of National Research Foundation under L2 NIC Award No.: L2NICCFP1-2013-7.

7. REFERENCES

[1] Y. Kajikawa, W. S. Gan, and S. M. Kuo, "Recent advances on active noise control: open issues and innovative applications," *APSIPA Transactions on Signal and Information Processing*, vol. 1, 2012.

[2] W. S. Gan, S. Mitra, and S. M. Kuo, "Adaptive feedback active noise control headset: implementation, evaluation and its extensions," *IEEE Transactions on Consumer Electronics*, vol. 51, no. 3, pp. 975–982, Aug 2005.

[3] T. Schumacher, H. Krüger, M. Jeub, P. Vary, and C. Beaugeant, "Active noise control in headsets: A new approach for broadband feedback anc," in *2011 IEEE International Conference on Acoustics, Speech and Signal Processing (ICASSP)*, May 2011, pp. 417–420.

[4] S. M. Kuo and D. Morgan, *Active Noise Control Systems: Algorithms and DSP Implementations*, John Wiley & Sons, Inc., New York, NY, USA, 1st edition, 1995.

[5] P. A. Nelson and S. J. Elliott, *Active control of sound*, Academic press, 1991.

[6] D. Shi, C. Shi, and W. S. Gan, "A systolic fxlms structure for implementation of feedforward active noise control on fpga," in *Signal and Information Processing Association Annual Summit and Conference (APSIPA), 2016 Asia-Pacific*. IEEE, 2016, pp. 1–6.

[7] J. Lorente, M. Ferrer, M. De Diego, and A. González, "Gpu implementation of multichannel adaptive algorithms for local active noise control," *IEEE/ACM Transactions on Audio, Speech and Language Processing (TASLP)*, vol. 22, no. 11, pp. 1624–1635, 2014.

[8] B. Lam, S. J. Elliott, J. Cheer, and W. S. Gan, "The physical limits of active noise control of open windows," in *12th Western Pacific Acoustics Conference*, December 2015.

[9] B. Lamand C. Shi and W. S. Gan, "Active Noise Control Systems for Open Windows : Current Updates and Future Perspectives," in *Proceedings of the 24th International Congress on Sound and Vibration*, London, UK, 2017, pp. 1–7.

[10] X. Qiu, "Recent advances on active control of sound transmission through ventilation windows," in *Proceedings of the 24th International Congress on Sound and Vibration*, London, UK, 2017.

[11] E. A. Wan, "Adjoint lms: an efficient alternative to the filtered-x lms and multiple error lms algorithms," in *1996 IEEE International Conference on Acoustics, Speech, and Signal Processing Conference Proceedings*, May 1996, vol. 3, pp. 1842–1845 vol. 3.

[12] D. Shi, J. He, C. Shi, T. Murao, and W. S. Gan, "Multiple parallel branch with folding architecture for multichannel filtered-x least mean square algorithm," in *2017 IEEE International Conference on Acoustics, Speech and Signal Processing (ICASSP)*, March 2017, pp. 1188–1192.

[13] R. Ranjan, T. Murao, B. Lam, and W. S. Gan, "Selective active noise control system for open windows using sound classification," in *INTER-NOISE and NOISE-CON Congress and Conference Proceedings*. Institute of Noise Control Engineering, 2016, vol. 253, pp. 1921–1931.

[14] B. Rafaely, "Active noise reducing headset-an overview," in *INTER-NOISE and NOISE-CON Congress and Conference Proceedings*. Institute of Noise Control Engineering, 2001, vol. 2001, pp. 2144–2153.

[15] P. Marek, "Analogue active noise control," *Applied Acoustics*, vol. 63, no. 11, pp. 1193 – 1213, 2002.

[16] A. V. Oppenheim and A. S. Willsky, *Signals and Systems (2nd Edition)*, Pearson Education Limited, 2014.

[17] S. S. Haykin, *Adaptive filter theory*, Pearson Education India, 2008.

[18] J. J. Shynk, "Frequency-domain and multirate adaptive filtering," *IEEE Signal Processing Magazine*, vol. 9, no. 1, pp. 14–37, Jan 1992.

[19] X. Li S. Liu and J. Tian, "Transform domain adaptive filter in active noise control," in *6th International Conference on Signal Processing, 2002.*, Aug 2002, vol. 1, pp. 272–275 vol.1.

[20] P. C. W. Sommen, "Partitioned frequency domain adaptive filters," in *Twenty-Third Asilomar Conference on Signals, Systems and Computers, 1989.*, Oct 1989, vol. 2, pp. 677–681.

[21] P. C. W. Sommen and E. de Wilde, "Equal convergence conditions for normal- and partitioned-frequency domain adaptive filters," in *[Proceedings] ICASSP-92: 1992 IEEE International Conference on Acoustics, Speech, and Signal Processing*, Mar 1992, vol. 4, pp. 69–72 vol.4.